

Simulation of a 3D Flow-Focusing Capillary-Based Droplet Generator

D. Conchouso*, E. Rawashdeh, A. Arevalo, D. Castro, I. G. Foulds
King Abdullah University of Science and Technology
4700 KAUST 23955, david.conchouso@kaust.edu.sa

Abstract: This paper presents the multiphase 2D axisymmetric simulation of a three-dimensional flow-focusing microfluidic droplet generator using the laminar two phase flow, phase field module in COMSOL Multiphysics®. The performance of the device is characterized at different flow conditions. The generation frequency and diameter of droplets was studied and shows direct correlation with the flow rates.

Keywords: Flow-focusing, droplet generator, capillary, microfluidics, water-in-oil droplets, COMSOL.

1. Introduction

Nowadays, droplet microfluidics is a continuously growing topic because it offers a completely new horizon for assays in the Pico-liter to Nano-liter size where miniaturization challenges such as: fluids evaporation, liquid handling, molecule adsorption and absorption had been an obstacle to further scale down scientific experiments [1].

By using droplets of immiscible fluids (typically water-in-oil W/O or oil in water O/W) researchers have been able to successfully accomplish reactions in contained volumes of reagents. Since droplets (also known as Disperse Phase DP) do not interact with the surrounding liquid (also known as Continuous Phase CP), the reactions can occur in an atmosphere clean of contaminations, chemical noise and controlled conditions (i.e. temperature, stoichiometry ratios, mixing) that can be manipulated at the level of a single droplet. Droplet microfluidics offer a new platform for chemical synthesis, and high-throughput screening of chemical, molecular and biological libraries [1-3].

Applications of this technology include single cell assays, drug and chemical encapsulation, gas-liquid reactions, point of care diagnostic devices, and synthesis of diverse materials such as: biomolecules, crystals, polymeric particles and nanoparticles [2], [4-6].

Different microfluidic droplet generators have been introduced to produce monodisperse droplets; however, in this paper we focus on a

capillary-based three-dimensional flow-focusing microfluidic droplet generator.

Capillary-based devices have become very popular within the microfluidics community due to features such as: greater flexibility to tune droplet's size by adjusting flow rates, higher monodisperse throughput, and stronger resistance to handle strong organic solvents and aggressive chemical reactions.

Another significant advantage of capillary-based devices compared to any other microfluidic droplet generators is the fact that they have no direct interaction with the microstructure's walls after the droplets are generated. This lack of interaction is due to the narrow focused-stream of disperse phase that is formed prior passing through the confinement orifice. Thus, the small droplets formed never touch the orifice walls, reducing the probability of the system to experience fouling problems, and improving its reliability. Because of the aforementioned advantages, capillary-based systems have been used to create single, double or triple emulsions for encapsulation of drugs, and fabrication of monodisperse vesicles, liquid crystal shells, and particles with different internal structures [7, 8]

These capillary-based flow-focusing systems are usually manufactured by manually assembling tapered glass capillaries on a square channel [4, 8]. Their fabrication process is laborious because of alignment and their characterization is time consuming, thus a model that can aid in their design is needed to grasp a better understanding of their dynamic behavior. Virtual testing is also much faster than doing several design iterations, running a fabrication process and then doing their characterization.

2. Capillary-Based Microfluidic Droplet Generator

In this work we will use COMSOL Multiphysics to characterize the performance of a 3D flow-focusing capillary-based microfluidic droplet generator in which the disperse phase (inner fluid) is hydro-dynamically flow focused in a 3D-space by an immiscible continuous fluid.

When both fluids are forced to pass through a narrow orifice, the disperse phase experiences elongation and finally droplet break up downstream.

The microfluidic droplet generator studied here is shown in Figure 1. It consists of a standard glass capillary tube with inner diameter of 508 μm that has a tapered reduction in diameter to form a 250 μm orifice over a 375 μm distance. The device has an axisymmetric input for the disperse phase and a ring-like input for the continuous phase.

The ring-like inlet emulates the entrance of the continuous phase from a square outer channel. The height of this ring is 500 μm and represents the thickness of the capillary tube.

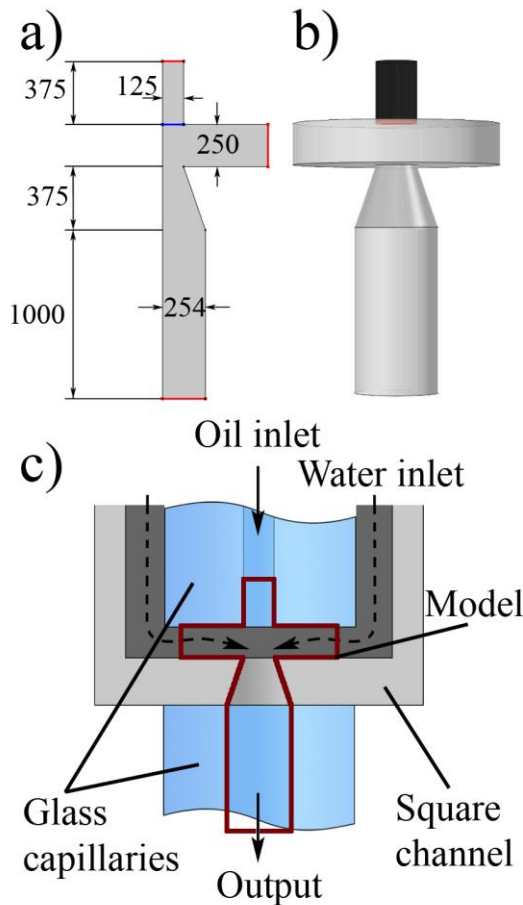


Figure 1. Diagram of the capillary-based microfluidic droplet generator. a) Top view 2D axisymmetric slice with dimensions. b) Solid of revolution formed by revolving the slice shown in a). c) Schematic of the assembly of a capillary-based MFDG from which our model was derived.

3. COMSOL Multiphysics® Laminar Two-Phase Flow, Phase Field Module.

We used the phase field method to study the interfacial motion of the multiphase flow. This method allows us to observe the geometric evolution of the fluidic interface with Eulerian formulation. In microfluidics, the devices normally face a laminar flow behavior due to their reduced size, therefore, the Laminar Two-Phase Flow, Phase Field module was selected to perform this simulation.

Although there are other methods like level set to simulate the laminar two-phase flow, the phase field method has a more robust coupling with other physics in COMSOL Multiphysics®. This advantage can be used to model several physics such as: chemical diffusion, heat transfer, electric field and other related phenomena involved with the system.

In the phase field method, the multiphase flow is described by the parameter ϕ . Here one fluid element is defined as $\phi = 1$, whereas the second fluid element is $\phi = 0$. The interface between them (phase field) is the set of values $1 < \phi < 0$.

The phase field module in COMSOL Multiphysics® uses the continuity equation in order to satisfy the condition of conservation of mass for the incompressible flow:

$$\nabla \cdot \mathbf{u} = 0$$

Where \mathbf{u} is the velocity vector.

In the same way it considers the conservation of momentum for an incompressible flow solving the Navier-Stokes equations to describe the fluid evolution in the multiphase system.

$$\begin{aligned} \rho \left(\frac{\partial \mathbf{u}}{\partial t} + (\mathbf{u} \cdot \nabla) \mathbf{u} \right) &= \nabla \cdot [-p\mathbf{I} + \mu(\nabla \mathbf{u} + \nabla \mathbf{u}^T)] \\ &+ \mathbf{F}_g + \mathbf{F}_{st} + \mathbf{F} \end{aligned}$$

Where \mathbf{u} is the velocity vector, p is the pressure, ρ is the density, μ is the dynamic viscosity, and \mathbf{F}_g is the gravitational force, \mathbf{F}_{st} is the surface tension force and \mathbf{F} are other external forces in the system.

The phase field method defines two tracking parameters, to describe the fluids' evolution. Where λ is the mixing energy density and ε is proportional to the interface thickness. These parameters are related by means of the surface tension in this simulation:

$$\sigma = \frac{2\lambda(2)^{1/2}}{3\varepsilon}$$

Finally, COMSOL Multiphysics® creates this relations:

$$\frac{\partial\phi}{\partial t} + u \cdot \nabla\phi = \nabla \cdot \frac{\gamma^\lambda}{\varepsilon} \nabla\psi$$

$$\psi = -\nabla \cdot \varepsilon^2 \nabla\phi + (\phi^2 - 1)\phi + \left(\frac{\varepsilon^2}{\lambda}\right) \frac{\partial f_{ext}}{\partial\phi}$$

A more detailed discussion of the theory related to the laminar phase field method can be found elsewhere [9], [10]

4. Simulation Setup

In these simulations, a 2D axisymmetric plane was used to draw the device, thus simplifying the complexity of the problem and reducing simulation run-times in comparison to drawing the full device in a 3D space, thus allowing for a rapid convergence. A physics-controlled mesh with free triangular geometry and a fine mesh were selected.

We used the fluid properties for Oil and water from the COMSOL Multiphysics® benchmark “Droplet-breakup” as inputs for our simulations. The surface tension between both fluid phases was set to $\sigma = 5$ mN/m, the contact angle was $\theta = 3\pi/4$, and the selected material properties are shown in Table 1.

Table 1. Fluid properties used in these simulations

Property	Oil (DP)	Water (CP)
Density (Kg/m ³)	1000	1000
Dynamic viscosity (mPa·s)	6.71	1.95

For both the phase initialization and the time dependent studies, a direct PARDISO solver was used. Time ranges were between 0 - 0.5 seconds

and time steps were in the range of 0.002 – 0.01 s depending on flow rates to be able to capture the evolution of the flow when the frequency of generation was high.

Figure 2 shows the boundaries that were defined as inlets and outlets for water and oil. Both inlets were set with a fixed flow rate, while the outlet was set to zero pressure with no viscous stress.

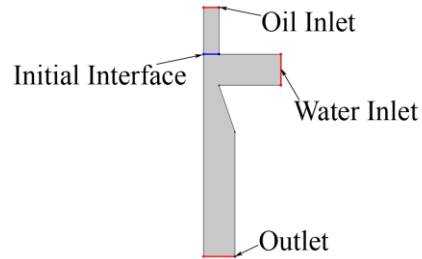


Figure 2. Boundary Conditions defined for the microfluidic droplet generator in the 2D axisymmetric model. The device has two inlets set with a constant flow rate. The outlet is set to have zero pressure with no viscous stress.

5. Simulations Results and Discussion

Figure 3 shows a typical behavior for droplet formation in this capillary-based device. First the disperse phase meets the continuous phase and forms a convex shape governed by the surface tension of the fluid. Then this interface grows until necking is formed because of the three-dimensional hydrodynamic focusing exerted by the viscous forces of the continuous phase. Finally droplet break up is generated to minimize the surface tension energy.

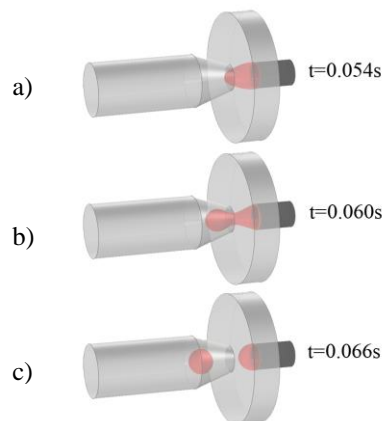


Figure 3. Typical time sequence for droplet generation at 15µl/min for both inlets, a) The DP meets the CP at the initial interface, b) Necking occurs by the focusing force of CP, and c) Droplet breakup.

Simulations were run at different total flow rates (15, 30 and 60 $\mu\text{l}/\text{min}$), and at different oil:water flow rate ratios (1:1, 1:1.5, 1:2), and the droplet diameter and generation frequency were measured.

For each flow rate configuration, the droplet diameter was obtained as follows. We performed a surface integration of the oil volume fraction along a section of the output channel. Because of the symmetry condition, the number obtained corresponds to half of a circle's surface, from which the diameter was calculated by:

$$D = 2 \sqrt{\frac{2 \cdot \text{Surface}}{\pi}}$$

The droplet diameters versus flow rate ratio, normalized to the channel's hydraulic diameter ($D_h = 250 \mu\text{m}$) are shown in Figure 4, top.

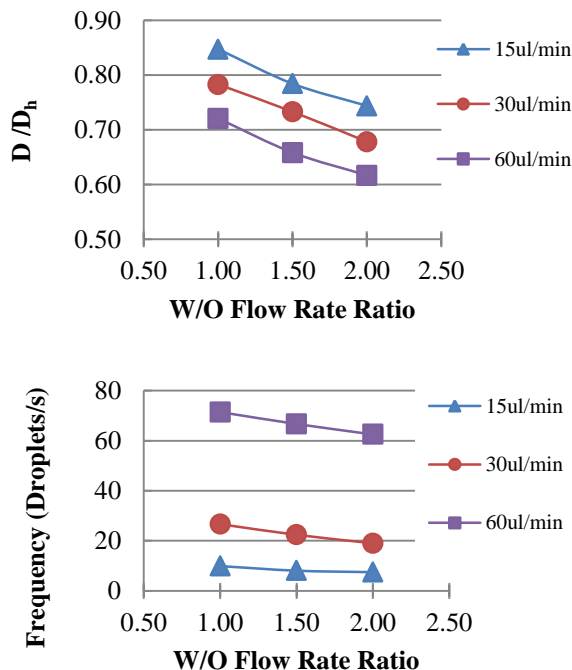


Figure 4. Top: Normalized droplet diameter (D/D_h) versus flow rate ratio, at different total flow rates. Bottom: Frequency of generation (in droplets per second) versus flow rate ratio, at different total flow rates.

The frequency of the droplet generation was simply obtained by counting the amount of droplets generated in a given sequence of frames, and then divided by the total time lapse, shown in Figure 4, bottom.

Droplet generation is determined by the balance between viscous forces, and interfacial tension of both phases. The dimensionless capillary number relates these concepts:

$$C_a = \frac{\mu \cdot U}{\sigma}$$

Where μ is the dynamic viscosity, U is the velocity vector and σ the interfacial tension. At high capillary numbers, the generated droplets are expected to be smaller due to the higher velocity, which increases the droplet-generating shearing forces. This behavior is in good agreement with our results, in which droplet size decreases by increasing either total flow rate or flow rate ratio. Similarly, when generating smaller droplets, a higher generation frequency is expected at a constant disperse phase flow.

Doubling the oil:water flow rate ratio, the droplet diameter decreased $\sim 15\%$ for the three total flow rates tested. Doubling the total flow rate has a smaller impact on droplet diameter, decreasing it by $\sim 10\%$.

The frequency of generation is highly dependent on total flow rate, in order to conserve the fixed disperse phase flow. The effect of changing the flow rate ratio also becomes more pronounced at higher total flow rates.

6. Conclusions

In this work we have successfully simulated a capillary-based micro fluidic droplet generator. We took advantage of the device's axisymmetric geometry to model it in a simpler 2D fashion, which reduces the solution time significantly (less than 15 minutes).

At small time increments in the time dependent study, it is possible to visualize the focusing behavior of the fluids during droplet formation.

A correlation was found between flow conditions, and droplet diameter and frequency of generation. At higher flow rates, droplet diameter decreases, and frequency of generation increases.

7. References

1. D. N. Breslauer, P. J. Lee, and L. P. Lee, "Microfluidics-based systems biology - Molecular BioSystems," *Molecular Biosystems*, (2006).
2. A. B. Theberge, F. courtois, Y. schaeferli, M. Fischlechner, C. Abell, F. Hollfelder, and W. T. S. Huck, "Microdroplets in Microfluidics: An Evolving Platform for Discoveries in Chemistry and Biology," *Small*, (2010).
3. H. Song, D. L. Chen, and R. F. Ismagilov, "Reactions in Droplets in Microfluidic Channels - Angewandte Chemie International Edition, (2006).
4. J.-T. Wang, J. Wang, and J.-J. Han, "Fabrication of Advanced Particles and Particle-Based Materials Assisted by Droplet-Based Microfluidics," *Small*, vol. 7, no. 13, pp. 1728–1754, (2011).
5. P. S. Dittrich and A. Manz, "Lab-on-a-chip: microfluidics in drug discovery" *Nature Reviews Drug Discovery*, (2006).
6. J. I. Park, A. Saffari, S. Kumar, A. Günther, and E. Kumacheva, "Microfluidic Synthesis of Polymer and Inorganic Particulate Materials," *Annu. Rev. Mater. Res.*, vol. 40, no. 1, pp. 415–443, (2010).
7. L.-Y. Chu, A. S. Utada, R. K. Shah, J.-W. Kim, and D. A. Weitz, "Controllable Monodisperse Multiple Emulsions," *Angew. Chem. Int. Ed.*, vol. 46, no. 47, pp. 8970–8974, (2007).
8. R. Shah, H. Shum, A. Rowat, D. Lee, J. Agresti, A. Utada, L. Chu, J. Kim, A. Fernandeznieves, And C. Martinez, "Designer emulsions using microfluidics," *Materials Today*, vol. 11, no. 4, pp. 18–27, (2008).
9. P. Yue, J. J. Feng, C. Liu, and J. Shen, "A diffuse-interface method for simulating two-phase flows of complex fluids," *Journal of Fluid Mechanics*, (2004).
10. Y. Sun and C. Beckermann, "Sharp interface tracking using the phase-field equation," *Journal of Computational Physics*, vol. 220, no. 2, pp. 626–653, (2007).